A quasi two-dimensional model for sound attenuation by the sonic crystals

A. Gupta,[a] K. M. Lim, and C. H. Chew
Department of Mechanical Engineering, National University of Singapore, Singapore 117576, Singapore

(Received 14 December 2011; revised 6 March 2012; accepted 19 March 2012)

Sound propagation in the sonic crystal (SC) along the symmetry direction is modeled by sound propagation through a variable cross-sectional area waveguide. A one-dimensional (1D) model based on the Webster horn equation is used to obtain sound attenuation through the SC. This model is compared with two-dimensional (2D) finite element simulation and experiment. The 1D model prediction of frequency band for sound attenuation is found to be shifted by around 500 Hz with respect to the finite element simulation. The reason for this shift is due to the assumption involved in the 1D model. A quasi 2D model is developed for sound propagation through the waveguide. Sound pressure profiles from the quasi 2D model are compared with the finite element simulation and the 1D model. The result shows significant improvement over the 1D model and is in good agreement with the 2D finite element simulation. Finally, sound attenuation through the SC is computed based on the quasi 2D model and is found to be in good agreement with the finite element simulation. The quasi 2D model provides an improved method to calculate sound attenuation through the SC.
 [http://dx.doi.org/10.1121/1.4744930]

PACS number(s): 43.20.MV [ANN] Pages: 2909–2914

I. INTRODUCTION

Sound propagation over a periodic arrangement of scatterers has been of interest over the past few decades. The initial study began with Martinez *et al.*[1] in 1995, when it was found that an artistic creation has possible engineering applications. The structure was based on a minimalistic design (an art movement in the 1950s based on simplistic forms and designs), consisting of hollow steel rods, 3 cm in the outer diameter, arranged on a square lattice with a lattice constant of 10 cm. When sound propagates through this structure, it was found that certain bands of frequencies are significantly attenuated compared to other frequencies. This finding led to increased interest among researchers to explore sound propagation through periodic structures. Periodic structures come in different configurations. When the medium of wave propagation (the host) is fluid and scatterers are solid (as in the present case) or vice versa, such structures are referred as sonic crystals (SCs). When both the host and scatterers are of the same media, such as solid in solid, these are known as phononic crystals.

It has been found that periodic structures do not behave homogeneously with respect to waves of all frequencies. Certain bands of frequencies can propagate through the structure, while certain bands of frequencies cannot propagate through the structure, which are referred to as bandgaps.[2] It should be noted that the bandgaps appear for an "infinitely periodic structure." Figure 1(a) shows a two-dimensional (2D) array of circular scatterers which extends infinitely. Such a structure is referred to as a periodic structure. For a periodic structure, sound does not propagate in the bandgap region. However, in practice, the structure is of finite size. Especially for sound waves in the audible frequency range, the size of the repeating unit is of the order of few centimeters, and the structure becomes large with a number of scatterers arranged periodically. It is therefore important to study not just the bandgap for a periodic structure but also the sound attenuation through the finite structure. For such a finite structure or SC, significant sound attenuation is observed in the frequency range corresponding to the bandgap. This is explained by the evanescent wave in the bandgap region due to a nonzero imaginary part of the wavenumber.[2] The sound attenuation is not due to absorption or viscosity in the model. The sound attenuation in the SC is due to the interference of the wave after passing through the periodic structure.

SCs have promising applications in engineering and science. Trees arranged in a periodic arrangement[3] gave better sound attenuation compared to a green belt or forest. The frequencies attenuated corresponded to the periodicity of the lattice, and the array of trees works like a SC. Hence it was proposed that these periodic arrays of trees can be used as green acoustic screens. Similarly, in another study,[4] periodic structures of size 1.11 m × 7.2 m with cylinders of diameter 16 cm were used as acoustic barriers. The results showed good agreement with those predicted by Maekawa[5] for barriers. It was further proposed that introducing holes or vacancies in the structure will improve the behavior of the sample as a noise barrier for low frequencies.[6,7] Hence, further studies and improvements on the design of such structures would be quite beneficial.

Although the above represent a few recent research studies on bandgap structures in the field of acoustics, such properties of periodic structures have been extensively studied in the 1970s and 1980s in relation to light waves

[a]Author to whom correspondence should be addressed. Electronic mail: apn.gpt@gmail.com

(photonic crystals),[8] elastic waves,[9] and matter waves.[10] Methods such as the plane wave expansion method[11–13] and the multiple scattering methods[14] were used for calculating the band structures. These methods were mainly developed for photonic crystals which are also applied to SCs and phononic crystals. Bandgaps have also been explained based on the spring mass system.[15]

In the present work, sound propagation through the SC is modeled by sound propagating through a waveguide. Sound propagating through a waveguide with a variable cross-sectional area can be represented by the Webster horn equation which is an approximate equation, with the assumption of uniform pressure across the cross-section. This reduces the problem to a one-dimensional (1D) model represented by an ordinary differential equation.

Some of the drawbacks of the Webster equation are that it assumes sound hard lining, there is no mean flow, and pressure is assumed to be uniform across the cross-section. In some of the recent studies on Webster horn equation,[16] Rienstra has used the perturbation method and method of slow variation to obtain the Webster equation for such cases. Rienstra has also generalized the derivation to ducts with non-uniform speed of sound, ducts with irrotational mean flow, and ducts with acoustic lining.

Martin[17] has obtained some generalization on the Webster horn equation for higher order variants using a power series for an axis-symmetric waveguide. He has obtained a hierarchy of 1D ordinary differential equations for an axis-symmetric waveguide. The equations were obtained by solving the Helmholtz equation using a power-series expansion method in a stretched radial coordinate. The lowest approximation turns out to be the Webster equation. In a similar way we have included a quadratic term to the Webster equation which serves our purpose of modeling sound propagation through the SC satisfactorily.

In the present work, we have considered sound propagation in the SC along the symmetry direction (ΓX) (Fig. 1). Since the structure is symmetric about the plane AB and CD, the structure can be reduced to a strip model as shown by the rectangle in Fig. 1(b). Further using the symmetry about the center line, the model is reduced to a waveguide problem [Fig. 1(c)]. In Sec. II A the modeling of sound propagation through a waveguide using the Webster horn equation is discussed. Section II B gives the 2D finite element simulation for the pressure field. Section III discusses the computation of sound attenuation by the SC over the frequency range of 500–6000 Hz. Results on sound attenuation obtained from the Webster horn equation model and finite element simulation show some agreement but there is a shift of ~500 Hz for the attenuation band frequencies. We have also compared these results with the experimental result.[2] In Sec. IV, we discuss the reason for this shift and present a quasi 2D model as an improvement to the 1D Webster horn equation. This model assumes a parabolic pressure profile over the cross-section, and the set of equations is derived from the weighted residual method. The results when compared with finite element results and experiment showed significant improvement over the Webster horn model.

II. SOUND PROPAGATION THROUGH THE SC ALONG A SYMMETRY DIRECTION

The problem considered is shown in Fig. 1(b). A planar sound wave propagates along the symmetry direction ΓX of an array of circular scatterers arranged periodically. Since the problem is symmetric about AB and CD, the model can be reduced to a strip model as shown by the rectangle in Fig. 1(b). We consider sound attenuation over five layers of scatterers, which reduces to an array of five scatterers. The model is further reduced by taking the symmetry about the center line to give a waveguide as shown in Fig. 1(c). The top and bottom surfaces including the cylinders are modeled as sound hard boundaries. There is a sound source at the inlet end, and radiation boundary condition is applied at the outlet end. The problem is effectively reduced to one of sound propagation through a symmetric waveguide as shown in Fig. 1(c). The first solution to this problem is obtained by using a 1D model based on the Webster horn equation.

A. Sound propagation through a waveguide: Webster horn equation

Sound propagating through a waveguide with a variable cross-sectional area is modeled by the Webster horn equation. The Webster horn equation considers the pressure to be a function of only the direction of wave propagation, and constant over the cross-section of the waveguide. This reduces the problem to a 1D model represented by an ordinary differential equation. The Webster equation[18,19] is given by Eq. (1),

$$\frac{d^2p(x,t)}{dt^2} = \frac{c^2}{S}\frac{d}{dx}\left(S\frac{dp(x,t)}{dx}\right), \tag{1}$$

where p is the acoustic pressure, c is the speed of sound, and S is the cross-sectional area of the waveguide.

Assuming that the pressure is harmonic in time,

$$p(x,t) = \mathrm{Re}\left(P(x)e^{i\omega t}\right), \tag{2}$$

where $P(x)$ is complex-valued amplitude and ω is the angular frequency of the propagating wave. For harmonic response, the Webster horn equation reduces to Eq. (3),

$$\frac{d^2P}{dx^2} + \frac{dP}{dx}\left(\frac{S'}{S}\right) + \frac{\omega^2}{c^2}P = 0, \tag{3}$$

where S' represents the first derivative of S with respect to x.

The above equation is discretized along the x-axis using the second-order finite difference method to obtain a system of linear equations. The radius of cylinders r is 1.5 cm and lattice spacing a is 4.25 cm [as shown in Fig. 1(c)]. The cross-section area function $S(x)$ is shown in Fig. 1(c) by the dashed line, although the area function $S(x)$ is continuous but its derivative is not continuous at the beginning and end of the cylinders. However, this issue can be overcome by approximating the derivative numerically which takes a

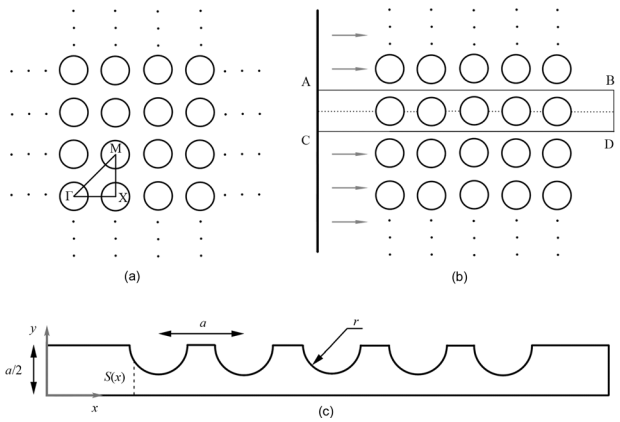

FIG. 1. (a) 2D periodic structure consisting of circular scatterers arranged periodically. (b) Plane wave propagating along the symmetry direction (ΓX) of a SC. Symmetry is used to reduce the model to a strip model shown by the rectangle. (c) A symmetric waveguide used for the quasi 2D model.

large numerical value. The results for sound attenuation (in dB) were checked for mesh convergence and thus the waveguide is suitably modeled numerically.

At the inlet node, a constant pressure boundary condition of 1 Pa was used, while at the outlet node a 1D Sommerfeld radiation boundary condition was used. The numerical results for pressure were found to converge for 2000 mesh points, for frequency up to 6000 Hz. The Helmholtz number for wave propagation given by ka varies from 0.38 to 4.67 in the frequency range of 500–6000 Hz.

B. Finite element method

To validate the results from the Webster equation model, finite element simulations were performed using the software COMSOL Multiphysics 3.4. A 2D model along with boundary conditions is shown in Fig. 2, consisting of an array of five circular scatterers with the same geometric parameters as mentioned before.

The pressure is assumed to be harmonic in time, and the wave propagation is modeled by the 2D Helmholtz equation given by Eq. (4),

$$\nabla^2 P(x,y) + \frac{\omega^2}{c^2} P(x,y) = 0, \tag{4}$$

where $p(x,y,t) = \mathrm{Re}(P(x,y)e^{i\omega t})$ and $P(x,y)$ is the complex amplitude.

For the finite element analysis, triangular quadratic elements (T6) were used for meshing the domain. The model

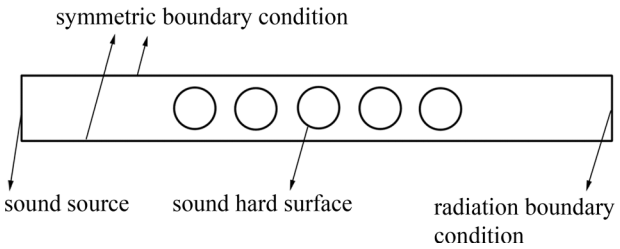

FIG. 2. Model used for the finite element simulation along with boundary conditions.

consists of 5004 elements, and the simulation was performed over a range of frequency from 500–6000 Hz in steps of 10 Hz. The simulation result was checked for convergence by using a finer mesh for the pressure field at the highest frequency of 6000 Hz. For the current model, the maximum element size is 5.6 mm, which was less than 1/10 of the wavelength at the highest frequency simulated (6000 Hz with a corresponding wavelength of 57 mm in air).

III. SOUND ATTENUATION BY THE SC FROM THE WEBSTER HORN MODEL AND FINITE ELEMENT SIMULATION

Sound attenuation by the SC is given by the insertion loss,

$$\mathrm{IL} = S\mathrm{PL}_{\text{without SC}} - \mathrm{SPL}_{\text{with SC}} \tag{5}$$

where $\mathrm{SPL}_{\text{without SC}}$ and $\mathrm{SPL}_{\text{with SC}}$ are the sound pressure levels at the same position without and with the SC, respectively. From both the models, sound pressure was measured 10 cm ($\sim 2.5\,a$) away from the last cylinder. As we will see in Sec. IV, sound pressure after and before the SC at this distance is mostly uniform across the cross-section, so that the y position of the point of measurement does not make a difference. The pressure amplitude obtained at this position corresponds to SPL with the SC ($\mathrm{SPL}_{\text{with SC}}$). When the cylinders are removed, the waveguide becomes a straight channel with uniform pressure amplitude across the cross-section, as the other end has radiation boundary condition. Therefore, the SPL without cylinders at the same position is the same as that corresponding to the incident wave amplitude when the cylinders are present.

Using the standard definition of SPL, the above expression for insertion loss reduces to

$$\mathrm{IL} = 20 \times \log 10\left(\frac{P_I}{P_O}\right), \tag{6}$$

where P_I is the amplitude of the inlet pressure wave that is incident on the SC and P_O is the amplitude of the outgoing pressure wave measured 10 cm after the last cylinder.

For the finite element model and the 1D model, a pressure boundary condition of 1 Pa was applied at the inlet. However, the prescribed pressure at the inlet boundary is not the forward traveling incident wave. This pressure at the inlet boundary is the result of a forward traveling incident wave and a backward traveling reflected wave. Pressure and velocity conditions at the inlet boundary were used to extract the incident pressure wave.

The pressure wave at the inlet is mostly 1D; hence, the net pressure can be written as a combination of forward and backward propagating wave,

$$p(x,t) = \mathrm{Re}\left\{P_I e^{i(\omega t - kx)} + P_R e^{i(\omega t + kx)}\right\} = \mathrm{Re}\{P(x)e^{i\omega t}\}, \tag{7}$$

therefore,

$$P(x) = P_I e^{-ikx} + P_R e^{ikx}, \tag{8}$$

where P_I and P_R are the amplitudes of the incident and reflected wave, respectively.

Similarly the velocity is given as[20]

$$u(x,t) = \mathrm{Re}\left\{\frac{1}{\rho c}\left(P_I e^{i(\omega t - kx)} - P_R e^{i(\omega t + kx)}\right)\right\} = \mathrm{Re}\{U(x)e^{i\omega t}\}, \tag{9}$$

where

$$U(x) = \frac{1}{\rho c}(P_I e^{-ikx} - P_R e^{ikx}). \tag{10}$$

At the inlet ($x = 0$), Eqs. (8) and (10) reduce to

$$P|_{x=0} = P_I + P_R, \tag{11}$$

$$U|_{x=0} = \frac{P_I}{\rho c} - \frac{P_R}{\rho c}. \tag{12}$$

The above set of simultaneous equations are solved to get the amplitude of incident forward traveling wave as a function of inlet boundary pressure P and velocity U at the boundary.

$$P_I = \left(\frac{P + \rho c U}{2}\right)\Big|_{x=0}. \tag{13}$$

The outgoing wave amplitude (P_O) can be directly obtained from the pressure field in the output region as there is no reflected wave in the output region.

In this way, sound attenuation at a particular frequency is obtained. The sound attenuation by the SC is independent of the applied pressure at the inlet. The procedure is repeated for a range of frequencies from 500–6000 Hz, with a frequency step of 10 Hz to obtain the sound attenuation by five cylindrical scatterers arranged periodically.

The results for the sound attenuation through the five circular scatterers are shown in Fig. 3. The results compare the sound attenuation obtained from the Webster horn equation and the finite element model along with our previous experimental result.[2] The experiment was conducted with five acrylic cylinders (similar to Fig. 2) and insertion loss was measured at the same location. For further details on experiment, please refer to our previous work.[2]

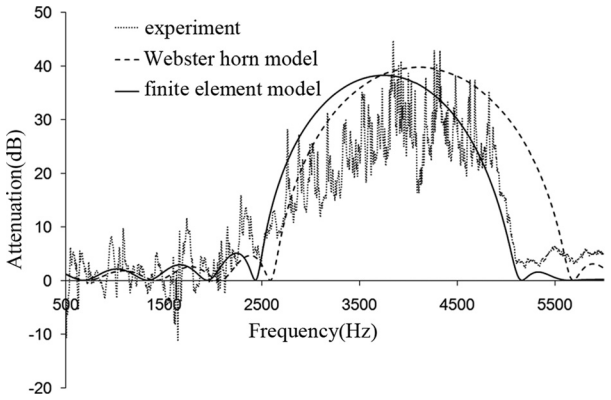

FIG. 3. Sound attenuation over five cylinders obtained from the Webster horn equation, finite element simulation, and experiment.

The sound attenuation results from the 1D model shows a significant sound attenuation (more than 20 dB) in the frequency range of 2900–5320 Hz, with a maximum sound attenuation of 39 dB. Finite element simulation predicts a significant sound attenuation in the frequency range of 2720–4820 Hz with a maximum sound attenuation of 38 dB. The two results also agree with the experimental results. Below 2500 Hz, there is no significant sound attenuation.

Although the results are in reasonable agreement, some observations can be made. The finite element results are much closer to the experimental results compared to the sound attenuation from the 1D model. Above 2500 Hz, the sound attenuation band from the 1D model is shifted to the right by about 200 Hz to 500 Hz at 2500 and 5000 Hz, respectively, compared to the experiment and the finite element model.

The reason for this frequency shift in sound attenuation band is due to the assumption of uniform pressure over the cross-section in the Webster horn equation. This assumption may hold true at low frequencies (for a low Helmholtz number) or when the cross sectional area is varying slowly. However, near the cylinders or for high frequencies, the pressure varies significantly in both directions, and hence this 2D behavior cannot be modeled effectively by the 1D model based on the Webster horn equation.

IV. QUASI 2D MODEL FOR SOUND PROPAGATION IN A WAVEGUIDE

The pressure variation in the SC can be studied through the finite element simulation and is shown in Fig. 4(a). Figure 4 shows the sound pressure in the strip model at 3500 Hz where the sound attenuation is quite significant (~37 dB). The pressure plot shows that there is a very feeble outgoing wave, and most of the incoming wave is attenuated by the SC. The frequency of high sound attenuation is chosen to observe the interaction of sound wave with the SC.

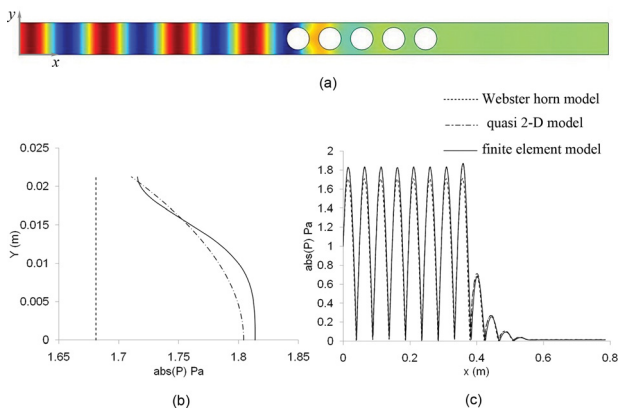

FIG. 4. (Color online) (a) Pressure plot in the strip model consisting of five circular scatterers at 3500 Hz. Pressure wave near the first and second cylinder is not uniform across the cross-section. (b) Pressure amplitude at a cross-section measured 0.5 cm before the first cylinder from different methods. (c) Pressure amplitude along the x-axis from different methods. The pressure amplitude from the finite element model overlaps with the quasi 2D model solution.

As can be seen in Fig. 4(a), sound pressure at a distance of even one unit cell a before and after the SC is uniform across the vertical cross-section. However, the pressure field near the cylinders is not uniform across the cross-sectional area. Therefore, the assumption in the Webster horn equation is certainly questionable. To improve upon the Webster horn equation, we have developed a method to include a non-uniform (parabolic) pressure profile across the cross-section.

The method is based on implementing the weighted residual method[21] on the 2D Helmholtz equation [Eq. (4)] for harmonic wave propagation. The residue of the Helmholtz equation is integrated over the cross-section, with y varying from 0 to $S(x)$. The pressure across the cross-section is assumed to be a linear combination of constant and parabolic pressure profile in the y direction as given by Eq. (14). The parabolic pressure profile is chosen so that the pressure is symmetric in the waveguide about the x axis [Fig. 1(c)],

$$P(x,y) = \alpha_0(x) + \alpha_1(x)y^2. \tag{14}$$

The Galerkin method is used so that the weighting functions are the same as the pressure profiles (1 and y^2). This leads to the weighted residual equations as

$$\int_0^{S(x)} \left\{ \frac{\partial^2 P(x,y)}{\partial x^2} + \frac{\partial^2 P(x,y)}{\partial y^2} + k^2 P(x,y) \right\} dy = 0, \tag{15}$$

$$\int_0^{S(x)} \left\{ \frac{\partial^2 P(x,y)}{\partial x^2} + \frac{\partial^2 P(x,y)}{\partial y^2} + k^2 P(x,y) \right\} y^2 dy = 0. \tag{16}$$

The above formulation results in two ordinary differential equations

$$\left(\bar{\alpha}_0'' + \frac{S'}{S}\bar{\alpha}_0' + k^2\bar{\alpha}_0 \right) + \frac{1}{S}\frac{d}{dx}\left((\bar{\alpha}_0 - P|_s)S' \right) = 0, \tag{17}$$

$$\left(\bar{\alpha}_1'' + \frac{3S'}{S}\bar{\alpha}_1' + k^2\bar{\alpha}_1 \right) + \frac{3}{S^3}\frac{d}{dx}\left((\bar{\alpha}_1 - P|_s)S^2S' \right) + \frac{6}{S^2}(\bar{\alpha}_0 - \alpha|_s) = 0, \tag{18}$$

where $\bar{\alpha}_0$ and $\bar{\alpha}_1(x)$ are pressure related quantities, defined in terms of coefficients of Eq. (14).

$$\bar{\alpha}_0(x) = \frac{\int_0^{S(x)} P(x,y)dy}{\int_0^{S(x)} dy} = \alpha_0(x) + \alpha_1(x)\frac{S^2}{3}, \tag{19}$$

$$\bar{\alpha}_1(x) = \frac{\int_0^{S(x)} P(x,y)y^2dy}{\int_0^{S(x)} y^2dy} = \alpha_0(x) + \alpha_1(x)\frac{3S^2}{5}. \tag{20}$$

Also, $P|_s$ is the pressure at top boundary, $y = S$,

$$P|_s = \alpha_0(x) + \alpha_1(x)S^2. \tag{21}$$

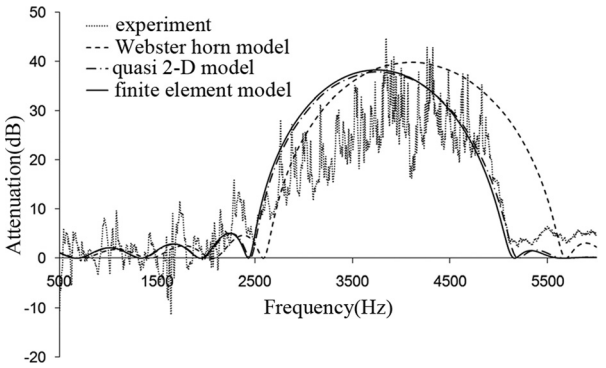

FIG. 5. Sound attenuation by an array of five circular scatters. Results comparing sound attenuation from the experiment, Webster horn model, quasi 2D model, and finite element model.

The above equations were solved simultaneously using the finite difference method to obtain values of $\alpha_0(x)$ and $\alpha_1(x)$. The pressure $P(x,y)$ is readily obtained using the quasi 2D model, for a given frequency.

It can be shown that when $\alpha_1(x) = 0$

$$P(x,y) = \alpha_0(x). \tag{22}$$

For this case, the quasi 2D model [Eqs. (17) and (18)] reduces to the Webster horn equation [Eq. (3)]. This shows that the Webster horn equation is a special case of the quasi 2D model.

The pressure obtained from the quasi 2D model and the Webster equation model is compared with the finite element simulation in Figs. 4(b) and 4(c). The results are compared at the frequency of 3500 Hz. Pressure amplitude across a vertical cross-section 0.5 cm before the first cylinder is plotted in Fig. 4(b). The result shows that there is a significant pressure variation across the cross-section. It clearly shows that the quasi 2D model is able to represent the 2D pressure variation better than the Webster equation model, as it is closer to the finite element results. Sound pressure along the x-axis is also compared in Fig. 4(c). Finite element results overlap with the quasi 2D model results. The comparison shows that quasi 2D model is a better representation than the original Webster equation.

Using the above quasi 2D model, sound attenuation is calculated for the range of frequencies from 500–6000 Hz. The sound attenuation curve for this model is closer to the finite element simulation and the experiment results than the Webster horn equation model (Fig. 5). This quasi 2D model predicts sound attenuation more accurately and does not exhibit the shift in frequency of the attenuation band as seen for the Webster equation model. This explains that the frequency shift in the attenuation band in the Webster equation model is due to the assumption of uniform pressure across the cross-section.

V. CONCLUSION

In the present work, we have considered sound propagation through the SC along the symmetry direction (ΓX). The symmetry in the structure is used to reduce the problem to a

waveguide model as shown in Fig. 1(c). Sound propagation through the waveguide is modeled by the Webster horn equation which assumes the pressure to be uniform over the cross-sectional area. This reduces a 2D problem to a 1D problem represented by a second order ordinary differential equation. The Webster horn equation model is used to obtain sound attenuation over a frequency range of 500–6000 Hz. Finite element simulation (2D) was performed for the same problem, and the results show a frequency shift (∼500 Hz) for the sound attenuation frequency range. The reason for this shift is due to the assumption of uniform pressure across the cross-sectional area in the Webster horn equation. We proposed a quasi 2D model which assumes the pressure as a linear combination of constant and parabolic pressure profile. The set of equations for this model is derived from the weighted residual method. The results are compared with finite element results, and it shows significant improvement over the Webster horn model.

The quasi 2D model can be used in other applications as an improved version of the Webster horn equation. The quasi 2D model can also be further extended to include higher order terms. However, for the present work on SCs, the parabolic term gives satisfactory results when compared with the finite element simulation. We can further use the quasi 2D model to recalculate the bandgap and obtain the decay constant for the SC. This may help us to improve the prediction of bandgaps for an infinite periodic structure.

The present models based on the Webster horn equation and quasi 2D model are valid only for wave propagating in one direction. The work can also be extended in the future for wave propagating in other directions.

[1]R. Martinez-Sala, J. Sancho, J. V. Sanchez, V. Gomez, J. Llinarez, and F. Meseguer, "Sound attenuation by sculpture," Nature **378**, 241 (1995).

[2]A. Gupta, K. M. Lim, and C. H. Chew, "Analysis of frequency band structure in one-dimensional sonic crystal using Webster horn equation," Appl. Phys. Lett. **98**, 201906 (2011).

[3]R. Martinez-Sala, C. Rubio, L. M. Garcia-Raffi, J. V. Sanchez-Perez, E. A. Sanchez-Perez, and J. Llinares, "Control of noise by trees arranged like sonic crystals," J. Sound Vib. **291**(1-2), 100–106 (2006).

[4]J. V. Sanchez-Perez, C. Rubio, R. Martinez-Sala, R. Sanchez-Grandia, and V. Gomez, "Acoustic barriers based on periodic arrays of scatterers," Appl. Phys. Lett. **81**(27), 5240–5242 (2002).

[5]Z. Maekawa, "Noise reduction by screens," Appl. Acoust. **1**(3), 157–173 (1968).

[6]V. Romero-Garcia, J. V. Sanchez-Perez, and L. M. Garcia-Raffi, "Propagating and evanescent properties of double-point defects in sonic crystals," New J. Phys. **12**, 083024 (2010).

[7]D. Caballero, J. Sanchez-Dehesa, R. Martinez-Sala, C. Rubio, J. V. Sanchez-Perez, L. Sanchis, and F. Meseguer, "Suzuki phase in two-dimensional sonic crystals," Phys. Rev. B **64**(6), 064303 (2001).

[8]E. Yablonovitch, "Inhibited spontaneous emission in solid-state physics and electronics," Phys. Rev. Lett. **58**(20), 2059–2062 (1987).

[9]M. M. Sigalas and E. N. Economou, "Elastic and acoustic-wave band-structure," J. Sound Vib. **158**(2), 377–382 (1992).

[10]C. Kittel, *Introduction to Solid State Physics* (Wiley, New York, 1971), p. 396.

[11]M. Kafesaki and E. N. Economou, "Multiple-scattering theory for three-dimensional periodic acoustic composites," Phys. Rev. B **60**(17), 11993–12001 (1999).

[12]M. M. Sigalas and E. N. Economou, "Attenuation of multiple-scattered sound," Europhys. Lett. **36**(4), 241–246 (1996).

[13]Y. I. Bobrovnitskii, "Impedance acoustic cloaking," New J. Phys. **12**, 043049 (2010).

[14]J. Mei, Z. Y. Liu, and C. Y. Qiu, "Multiple-scattering theory for out-of-plane propagation of elastic waves in two-dimensional phononic crystals," J. Phys. Condens. Matt. **17**(25), 3735–3757 (2005).

[15]J. S. Jensen, "Phononic band gaps and vibrations in one- and two-dimensional mass-spring structures," J. Sound Vib. **266**(5), 1053–1078 (2003).

[16]S. W. Rienstra, "Webster's horn equation revisited," SIAM J. Appl. Math. **65**(6), 1981–2004 (2005).

[17]P. A. Martin, "On Webster's horn equation and some generalizations," J. Acoust. Soc. Am. **116**(3), 1381–1388 (2004).

[18]A. G. Webster, "Acoustical impedance, and the theory of horns and of the phonograph," Proc. Natl. Acad. Sci. U.S.A. **5**, 275–282 (1919).

[19]A. H. Benade and E. V. Jansson, "On plane and spherical waves in horns with nonuniform flare—1. Theory of radiation, resonance frequencies, and mode conversion," Acustica **31**(2), 79–98 (1974).

[20]A. R. Frey and L. E. Kinsler, *Fundamental of Acoustics*, 3rd ed. (John Wiley and Sons, San Francisco, CA, 1982), p. 480.

[21]O. C. Zienkiewicz, R. L. Taylor, and J. Z. Zhu, *The Finite Element Method Set*, 6th ed. (Butterworth-Heinemann, Oxford, 2005), pp. 54.